ELSEVIER

Materials Chemistry and Physics 53 (1998) 172–178

MATERIALS CHEMISTRY AND PHYSICS

Growth of $MgWO_4$ phosphor by RF magnetron sputtering

J.P. Chu [a,*], I.J. Hsieh [b], J.T. Chen [c], M.S. Feng [d]

[a] Institute of Materials Engineering, National Taiwan Ocean University, Keelung, Taiwan
[b] Department of Electrical Engineering, Ching-Hua Polytechnic Institute, Hsingchu, Taiwan
[c] Institute of Materials Engineering, National Taiwan Ocean University, Keelung, Taiwan
[d] Institute of Materials Science and Engineering, National Chiao Tung University, Hsingchu, Taiwan

Received 13 May 1997; received in revised form 28 November 1997; accepted 17 December 1997

Abstract

Magnesium tungstate ($MgWO_4$) thin film phosphors prepared by radio frequency (RF) magnetron sputter deposition were characterized. α- and β-$MgWO_4$ were determined as the major phases in the films studied. Since the deposition rates of film were influenced by RF power, working pressure as well as oxygen content, these processing parameters played an important role in affecting the phase present in the as-deposited films. It is found that the formation of α-$MgWO_4$ phase was favorable for the films grown at low deposition rates (<40 Å min^{-1}) whereas β-$MgWO_4$ was a dominant phase at high deposition rates. Substrate temperatures showed no detectable effects on the deposition rates and thus the β-$MgWO_4$ was the only phase present for the substrate temperature range examined. A phase formation mechanism due to the deposition rate difference is described. Post-deposition annealing significantly improved the cathodoluminescence (CL) properties of films, with annealing temperatures at 750°C or above being the most effective. CL property improvement appeared to be attributed to the enhancement of crystallinity and the transformation to the stable β-$MgWO_4$ phase during the annealing. Annealing-induced film delamination and blisters, however, resulted in deterioration of low voltage CL properties. © 1998 Elsevier Science S.A. All rights reserved

Keywords: Phosphor; RF magnetron sputtering; Magnesium tungstate

1. Introduction

Phosphors are one of the most important materials that have been widely used to date in a number of applications such as displays and monitors. Powder phosphors are found to have many problems, e.g. contamination, poor adhesiveness and short service life. Phosphors in thin film form are thus considered for advanced applications, namely the field emission display. Most of the recent studies concerned with thin film phosphors were limited to the sulfides, for example rare earth-doped ZnS [1]. As decomposition of sulfides could, however, release sulfide gases and result in severe deterioration of phosphor properties as well as contamination of cathode filament [2,3], alternatives of sulfide phosphors have been considered. In the literature, there are reports of studies on $ZnGa_2O_4$ powder [3] and thin film [4,5] phosphors to be used for substituting blue cathodoluminescent (CL) sulfide-based phosphors. Yet, for the magnesium tungstate ($MgWO_4$) phosphor, another efficient blue CL material [6–8], very little attempt has been done in the thin film form.

$MgWO_4$ has been reported to have two distinct phases, commonly denoted as α and β-phases. α-$MgWO_4$ with a triclinic structure is a high temperature phase existing only at above 1250°C [7] or 1165°C [9], while β-$MgWO_4$ is a monoclinic phase and stable at low temperatures [7]. The β-$MgWO_4$ phase is a blue luminescent phosphor [7,8]. On the contrary, the high-temperature α-$MgWO_4$ phase does not show the luminescence at room temperature [7,8]. Accordingly, the luminescence property of $MgWO_4$ phosphor is strongly dependent upon the phase present. It is thus interesting to examine how thin film processing can produce $MgWO_4$ phosphors with a desired luminescence property. This study was directed toward characterizations of $MgWO_4$ thin films prepared by radio frequency (RF) magnetron sputter deposition in order to establish a fundamental understanding of processing variable effects on film properties and crystal structures. The processing parameters in terms of sputtering variables and post-deposition annealing conditions were optimized to attain $MgWO_4$ thin film phosphors with better luminescence property.

* Corresponding author. Tel.: +886-2-24622192; fax: +886-2-24625324; e-mail: b1085@ntou66.ntou.edu.tw

0254-0584/98/$19.00 © 1998 Elsevier Science S.A. All rights reserved
PII S0254-0584(98)00006-6

2. Experimental

For the sputter deposition, $MgWO_4$ powder target was synthesized. 1.5 part in weight of MgO and 1 part of WO_3 powder were ball-milled with alcohol for 24 h, followed by drying at 80°C and firing at 1150°C for 3 h in air. Excess MgO was dissolved by 3% HCl solution after firing. As-fired $MgWO_4$ powder target was pressed into a 7.5 cm dish for the thin film deposition. An RF magnetron sputtering system with a base pressure of $<5\times10^{-3}$ mTorr was used for the thin film deposition. Substrates were p-type silicon wafers and were cleaned prior to the deposition according to the standard RCA procedure. Argon was used as a working gas and oxygen as an active gas to obtain stoichiometric $MgWO_4$ thin film phosphors. For each deposition, 10 min presputtering of target was performed. Sputtering parameters studied included RF power, oxygen content, working pressure and substrate temperature. Deposition conditions of $MgWO_4$ thin film phosphors are listed in Table 1.

In order to study crystal structure change and to obtain better luminescence properties of the film, post-deposition annealing treatments were performed. The annealing was conducted in vacuum ($<8\times10^{-3}$ mTorr) at various temperatures for 2 h. Phase identifications of $MgWO_4$ powder and thin films were carried out by an X-ray diffractometer (XRD, Siemens D5000) with monochromatic CuK_α radiation at room temperature. Morphology and microstructure were characterized by field emission scanning electron microscopy (SEM, Hitachi S-4100). A scanning electron microscope (ABT 150S) equipped with a cathodoluminescence (CL) system was used at room temperature for the emission spectra measurements. Except for those low voltage measurements, CL was operated at 15 kV.

Table 1
Deposition conditions for $MgWO_4$ thin film phosphors

Conditions	Operation range
RF power	50–200 W
Working pressure	4–10 mTorr
Oxygen content	0–20%
Substrate temperature	unheated–450°C
Ar flow rate	20 sccm
Deposition period	120 min

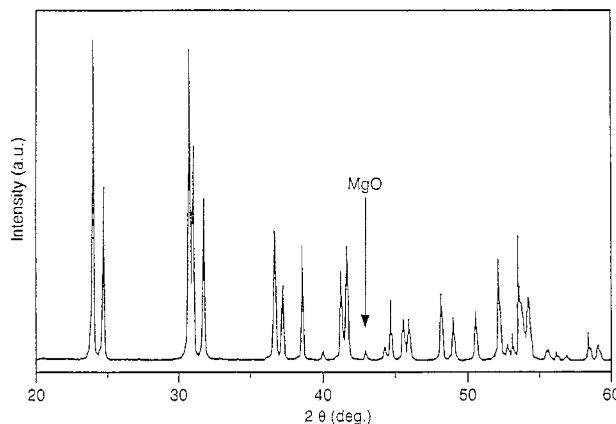

Fig. 1. XRD pattern of $MgWO_4$ powder target synthesized in this study.

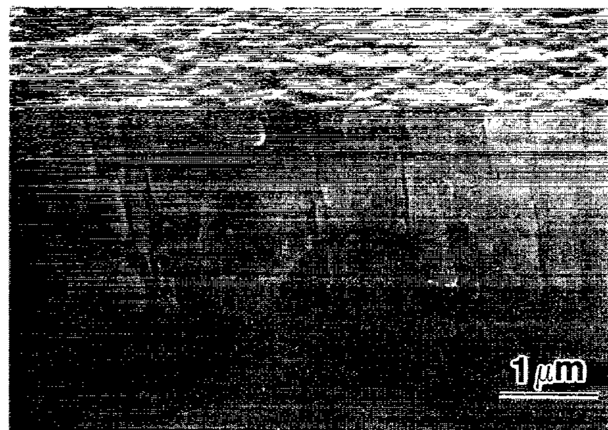

Fig. 2. SEM image of as-deposited film grown at 4 mTorr, 200 W, 10% O_2 and 450°C.

3. Results and discussion

3.1. Sputter deposition

Fig. 1 shows an XRD pattern of powder target synthesized in this study. The β-$MgWO_4$ phase was identified in the pattern as a major phase. The presence of a minor MgO peak in the pattern is presumably because the excess MgO was not completely dissolved and removed by HCl solution after target synthesis. Fig. 2 shows an SEM micrograph of an as-deposited film grown at 4 mTorr, 200 W, 10% O_2 and 450°C. Uniform and dense columnar film structure are observed from this micrograph. The composition of the powder target was 19 at.% Mg, 21% W and 60% O, while that of as-deposited $MgWO_4$ films was 15% Mg, 28% W and 57% O, as analyzed by an X-ray photoelectron spectrometer. There were no apparent variations in composition among the films containing $MgWO_4$ as the major phase. Deposition rates of films as functions of various processing parameters (RF power, oxygen content, working pressure and substrate temperature) are shown in Fig. 3. It is shown that the deposition rate increased monotonically with RF power while it increased with decreasing working pressure or oxygen content. The gradual decrease in deposition rate with increasing oxygen content is mainly related to the less efficient sputtering ion (Ar^+) concentration [10]. Substrate temperature effects on the deposition rate is not significant. As will be described below, film grown under various deposition conditions yielded different crystal structures and thus the deposition rate played a dominant role in the formation of film crystal structure.

The effect of RF power on as-deposited film crystallography is shown in XRD patterns of Fig. 4. The diffraction patterns were taken from films prepared with a condition of 4 mTorr, 10% O_2, and 450°C. When the film was formed at

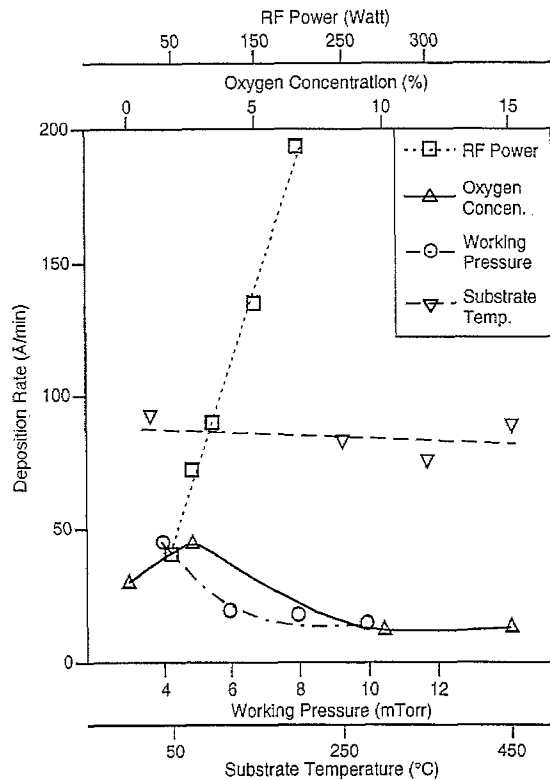

Fig. 3. Deposition rates of films as functions of various processing parameters: RF power, oxygen content, working pressure, and substrate temperature.

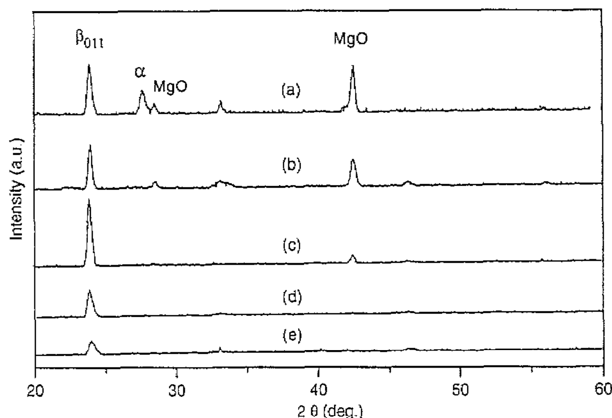

Fig. 4. XRD patterns of as-deposited films prepared at different RF powers: (a) 50, (b) 75, (c) 100, (d) 150, and (e) 200 W (4 mTorr, 10% O_2 and 450°C).

50 W, both MgO and the high-temperature α-$MgWO_4$ phase were present in addition to the β-$MgWO_4$ phase. The former two phases diminished with the β-$MgWO_4$ becoming a major phase as the RF power increased. Since the RF power raised the film deposition rate (Fig. 3), this indicates that the β-$MgWO_4$ phase with (011) preferred orientation was developed for the films grown at the higher deposition rates. In addition, an unidentified phase at ~33° of 2θ was found present at 50 and 75 W. The appearance of this phase seemed to be associated with MgO and they both vanished when high powers were applied. The effect of oxygen content on the as-deposited film crystallography is depicted in the XRD patterns of Fig. 5. These films were deposited at 4 mTorr, 50 W and 450°C. This figure reveals that when minimal oxygen was supplied only β-$MgWO_4$ and MgO existed in the films. The α-$MgWO_4$ phase, on the contrary, became predominant as the oxygen concentration increased. During the sputtering process, when the oxygen was not supplied neither α- nor β-$MgWO_4$ was formed. Instead, only MgO was present in the film. In addition, the deposition rate showed a decreasing trend as the oxygen contents increased, as indicated in Fig. 3, suggesting that the β-$MgWO_4$ formed at higher deposition rates, consistent with the RF power effects. To study further how the deposition rate influenced the β-$MgWO_4$ phase formation, working pressure effects were examined. Fig. 6 shows a series of XRD patterns obtained from as-deposited films grown under different working pressures, but at the same condition of 50 W, 10% O_2, and 450°C. As seen in this figure, the α-$MgWO_4$ phase diminished with decreasing working pressure while the β-$MgWO_4$ phase appeared to be a stable phase as the working pressure decreased. At low working pressures (e.g. 4 and 2 mTorr), the MgO phase coexisted with β-$MgWO_4$. It is shown in Fig. 3 that the deposition rate increased with decreasing working pressure. Therefore, in an agreement with the above results, the β-

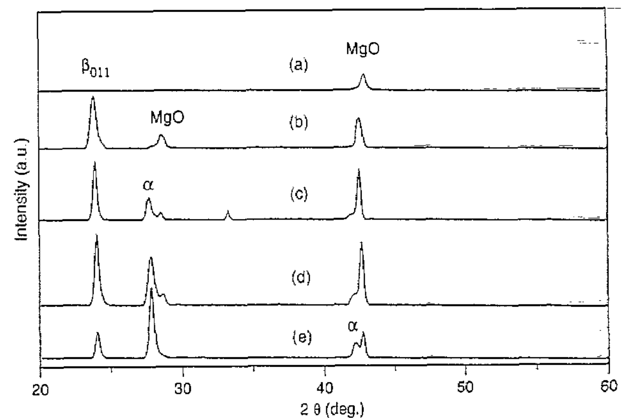

Fig. 5. XRD patterns of as-deposited films prepared at different oxygen contents: (a) 0%, (b) 2.5%, (c) 10%, (d) 15%, and (e) 20% O_2 (4 mTorr, 50 W and 450°C).

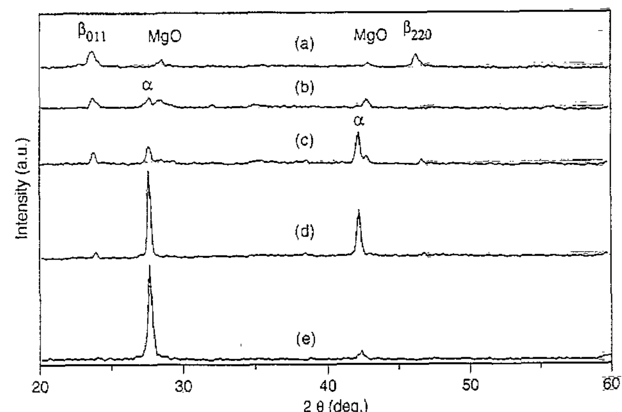

Fig. 6. XRD patterns of as-deposited films prepared at different working pressure: (a) 2, (b) 4, (c) 6, (d) 8, and (e) 10 mTorr. (10% O_2, 50 W and 450°C).

$MgWO_4$ phase was likely to form when the working pressure decreased or when the film grew at the relatively greater rates.

In order to understand the influence of the deposition rate on the formation of the α- or β-$MgWO_4$ phase, the growth mechanism of sputtered films is considered. In the sputter deposition process, Ar ions and other high-energy species bombard the target and transfer energy to the ejected atoms as well as generate heat. Before arriving at the substrate surface, the sputtered atoms are at a high-temperature state. Compared to the sputtered atoms, the substrate is so cool that it provides as a heat sink when the sputtered atoms deposit. The time required for an arriving atom to energetically equilibrate with substrate is estimated to be on the order of 10^{-12} seconds. Assuming an energy of 0.1 eV, which is equivalent to a temperature of 1000°C, this results in an effective quenching rate approaching 10^{15} °C s^{-1} [11]. Prior studies have shown that this quenching rate allows non-equilibrium atomic arrangements to be readily quenched-in, producing alloy films with compositions or structures which normally would not be allowed according to bulk thermodynamic constraints [12–15]. For instance, Cu–C 'pseudo-alloy' films can be formed by sputtering due to such high cooling rates by forced combinations of Cu and C elements which have essentially zero mutual solid or liquid solubilities [12].

In this study, XRD results, along with relationships given in Fig. 3, strongly suggest that the deposition rate played an important role in the phase formation. When the deposition rate was relatively low, below ~40 Å min^{-1}, the cooling rate effects were significant presumably because of the substrate not being heated-up and the high-temperature α-$MgWO_4$ phase formed favorably. Conversely, the low-temperature β-$MgWO_4$ phase likely formed when the film grew faster (above ~40 Å min^{-1}) due to a 'warm-up' effect of substrate from which many more high-temperature sputtered species arrived. This 'warm-up' effect is considered to be an in-situ annealing and analogy to that of the post-deposition annealing, which eventually leads to the formation of an equilibrium phase in the films, as discussed in the following section. Such an in-situ annealing effect has been demonstrated as well by Chu et al. in sputtered Cr thin films [16]. They found the equilibrium BCC Cr phase favorably formed when the film grew faster because the in-situ annealing of the film during deposition became increasingly influential. In the present study, the formation of the β-$MgWO_4$ phase in the films yielded better CL properties, as will be described later. Thus, the deposition rate of thin films affects their phase formations and of course their CL properties. Similar results have been reported earlier for ZnS:Mn thin films by Kawashima et al. [17]. They found that the luminous efficiency of eletroluminescence properties was enhanced by decreasing the deposition rate due to changes in the film surface roughness. In addition, other studies on $ZnGa_2O_4$ thin film phosphors also reported that the high deposition rates enhanced the crystallinity of films as well as improved luminescent properties [4,5]. Accordingly, luminescent properties of thin film phosphors were significantly influenced by the deposition rates through modifications of microstructure, crystallinity and phases in the films.

To verify the deposition rate effects, the substrate temperature was varied to examine its role on the crystallography of as-deposited films. In Fig. 7 XRD patterns were taken from films prepared at 4 mTorr, 10% O_2 and 100 W at different substrate temperatures. The XRD results show that the films were primarily of β-$MgWO_4$ phase for the substrate temperature range studied. Since deposition rates were above 40 Å min^{-1} and did not show noticeable variations with substrate temperatures studied (Fig. 3), one phase was expected to be present in the films according to the mechanism proposed earlier. In addition, when the substrate temperature was elevated the cooling rate decreased, facilitating formation of the β-$MgWO_4$ phase. Yet, changes in appearance of XRD patterns due to different substrate temperatures are noted. Bragg peaks appeared to shift to the high angle side when the substrate temperature increased. This similar phenomenon was also found when the high temperature annealing was applied, as is discussed later. Changes in d-spacing of the β-$MgWO_4$ phase at high temperatures are considered to be related to a lattice relaxation in the films. Further, it is noted that the intensities of β_{020} and β_{220} peaks both deceased in relation to that of the β_{011} peak as the substrate temperature increased, eventually resulting in formation of the β-$MgWO_4$ phase with (011) preferred orientation. Since the low-index crystallographic planes have relatively low surface energies, in cases where a more or less random orientation has been achieved for nucleation these planes will have favored growth rates than those of the high-index crystallographic planes [18]. As an increase in the substrate temperature will promote achievement of such random nucleation, growth of the low-index preferred orientation crystal structure is expected. In fact, similar results have been reported previously by Hsieh et al. [4,5] in $ZnGa_2O_4$ thin film phosphors prepared by RF magnetron sputtering. Their XRD patterns showed that the (222) peak diminished while the (311) and (220) peaks evolved as the substrate temperature increased to 600°C.

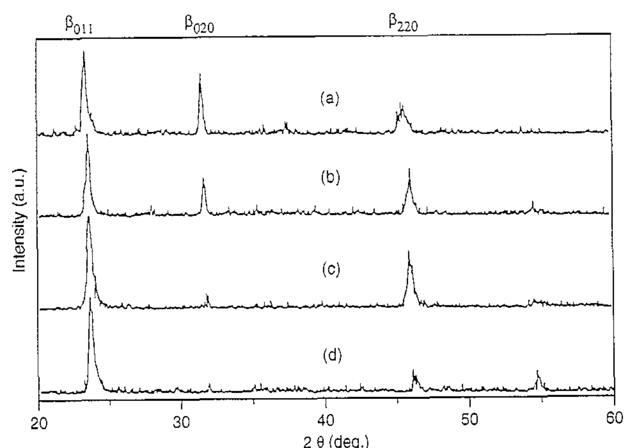

Fig. 7. XRD patterns of as-deposited films prepared at different substrate temperatures: (a) unheated, (b) 250°C, (c) 350°C, and (d) 450°C (4 mTorr, 10% O_2 and 100 W).

3.2. Post-deposition annealing

A series of XRD patterns of $MgWO_4$ films annealed at different temperatures for 2 h is shown in Fig. 8. Before annealing, these films predominantly of the β-$MgWO_4$ phase were deposited at a condition of 4 mTorr, 10% O_2, 100 W, without substrate heating. As seen from these XRD patterns, Bragg peaks of β-$MgWO_4$ appeared to displace to the high angle side as the annealing temperature increased up to 750°C. similar to those observed when the substrate temperature increased. Prior studies on $ZnGa_2O_4$ phosphor thin films also showed such peak shift to the high angles as the substrate temperature raised or the annealing was applied [4,5]. This behavior presumably was due to the stress relaxation induced by the high temperature of the substrate or the annealing. In addition, it is noted in this figure that a minor peak of the α-$MgWO_4$ phase was found present in the film after annealing at 750°C while the β-phase was fully developed at 850°C and the presence of the α-phase was not evident. A strong β_{020} peak is observed, indicating the (020) preferred orientation of the β-phase was developed after 850°C annealing. In contrast to the as-deposited films, the film annealed at 850°C for 2 h had a film crystal structure which resembled that of the target prepared (see Fig. 1).

In Fig. 9 X-ray results show the effects of annealing temperature on α-$MgWO_4$ films. Before annealing, these films mainly with the α-$MgWO_4$ phase were initially prepared at 10 mTorr, 50 W, 10% O_2, and 450°C, followed by annealing at various temperatures for 2 h. Similarly, Bragg peaks of α-$MgWO_4$ in the film shifted to the high angle side after annealing at 650°C, presumably due to the stress relaxation. At this temperature, the β-$MgWO_4$ phase began appearing. Annealing at temperatures at or above 750°C resulted in the formation of the β-$MgWO_4$ as the major phase. From Figs. 8 and 9, it is confirmed that regardless of the phases present in as-deposited conditions the high-temperature annealing has promoted the phase transformation, resulting in a thermodynamically stable phase with better crystallinity at room temperature. This stable phase, β-$MgWO_4$, is very similar to that of the powder target. As will be shown below, such phase transformation and crystallinity enhancement which occurred during the annealing is very beneficial in improving the cathodoluminescence property of $MgWO_4$ thin films.

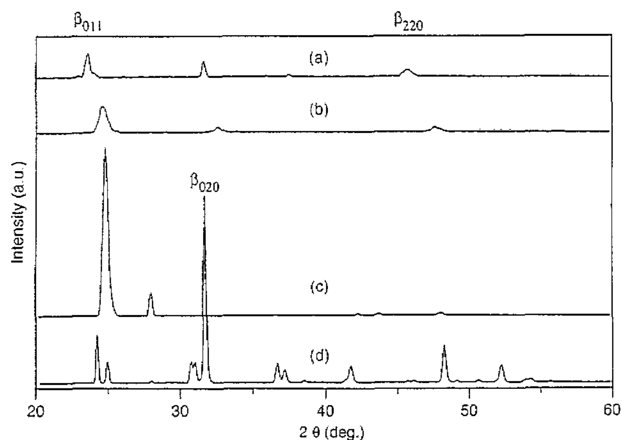

Fig. 8. XRD patterns of films annealed at various temperatures for 2 h: (a) as-deposited, (b) 650°C, (c) 750°C, and (d) 850°C. The films were initially β-$MgWO_4$ phase and grown at 4 mTorr, 10% O_2, and 100 W without substrate heating.

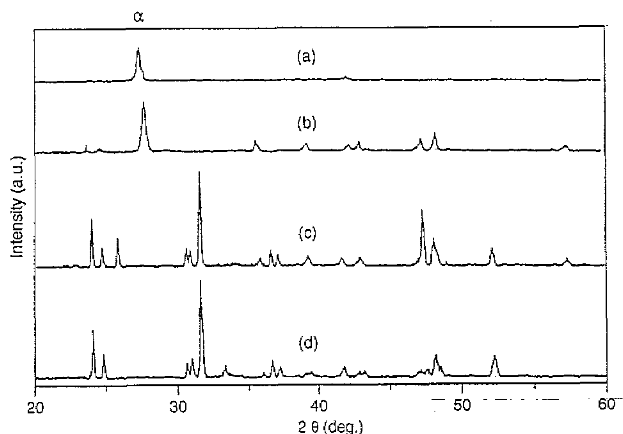

Fig. 9. XRD patterns of films annealed at various temperatures for 2 h: (a) as-deposited, (b) 650°C, (c) 750°C, and (d) 850°C. The films were initially α-$MgWO_4$ phase and grown at 10 mTorr, 10% O_2, 50 W, and 450°C.

Considering effects of annealing temperature on cathodoluminescence property, a series of spectra is shown in Fig. 10 (4 mTorr, 100 W, 10% O_2, and no substrate heating). As the annealing temperature increased, a noticeable increase of blue light intensity peaked at ~470 nm is observed and such intensity increase is prominent after annealing at 850°C. In

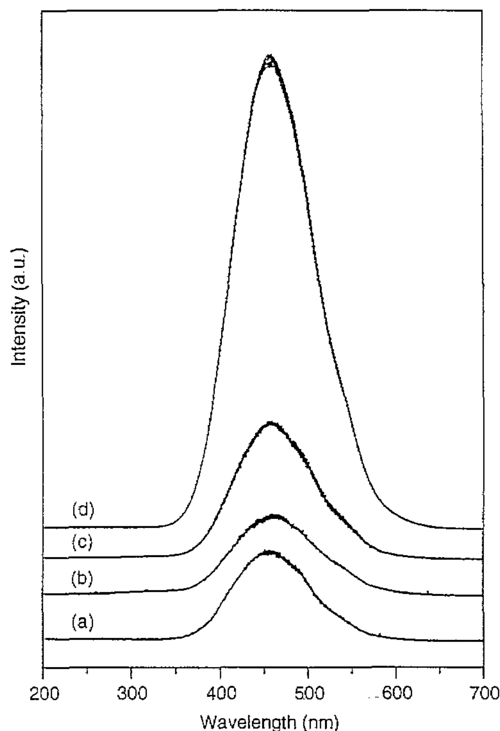

Fig. 10. Cathodoluminescence intensity as a function of annealing temperatures: (a) as-deposited, (b) 650°C, (c) 750°C, and (d) 850°C. The accelerating voltage was 15 kV. The films were initially β-$MgWO_4$ phase and grown at 4 mTorr, 100 W, and 10% O_2, without substrate heating.

literature, post-deposition annealing processes have been reported to greatly improve efficiency and brightness of the luminescence property for a number of thin film phosphors [4,5,19]. While the mechanisms for luminescence properties improvement are not necessarily the same, they are somewhat related to the modification of microstructure or enhancement of crystallinity of films. In this study, the luminescence property improvement is closely associated with the occurrence of the phase formation and better film crystallinity of β-$MgWO_4$. From XRD results of Figs. 8 and 9, it was found that the increase in cathodoluminescence intensity was well corresponded with the evolution of β-$MgWO_4$. According to the works by Kröger [7] and Blasse et al. [8], β-$MgWO_4$ is known to be a very efficient luminescent material and α-$MgWO_4$ does not show the luminescence at room temperature. Their results are in an excellent agreement with our findings. Accordingly, it is concluded that the improvement of film crystallinity and the transformation to equilibrium β-$MgWO_4$ phase by an annealing treatment could substantially improve the film luminescence property.

Because the low voltage cathodoluminescence (LVCL) is a very essential characteristic for the phosphors to be used in the field emission displays, LVCL properties of $MgWO_4$ film were investigated. Fig. 11 shows the room-temperature CL spectra of $MgWO_4$ films (4 mTorr, 100 W, 10% O_2, and no substrate heating) under different accelerating voltages. No significant peaks appeared at 1 kV, but blue light peaks were observed on the spectra under 15, 10 and 5 kV. In order to understand the detrimental LVCL property, the microstructure of the films were examined. Fig. 12 shows SEM images of the $MgWO_4$ film (4 mTorr, 100 W, 10% O_2, and no substrate heating) taken after annealing at 850°C was applied. In Fig. 12(a), a planar-view low-magnification SEM image reveals many craters as well as blisters present and some portions of substrate being exposed as a result of annealing. A cross-sectional high-magnification SEM image in Fig. 12(b) shows that the structure of the film after annealing was not apparently dense and some voids were clearly seen at the interface region. Formation of voids is not well understood at present. However, it might be a result of inter-diffusion of atoms between the substrate and film during annealing. The voids at the interface region could consequently cause the poor adhesion of the film, ultimately giving rise to delamination and formation of craters seen in Fig. 12(a). Deterioration of the LVCL property was thus considered to be attributed to these annealing-induced defects.

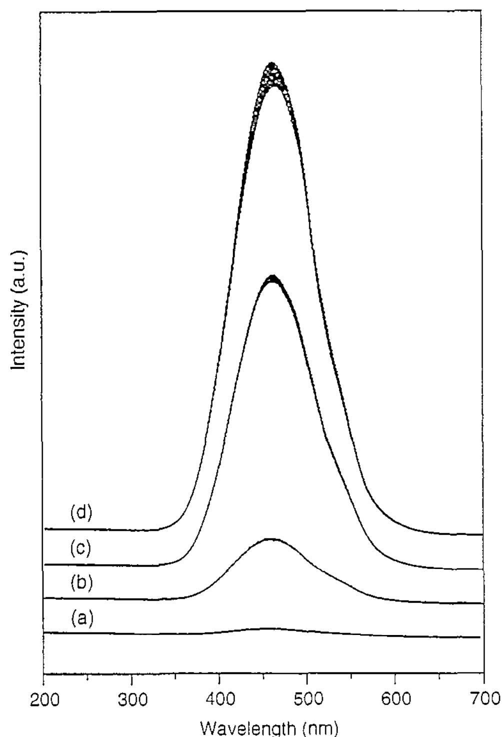

Fig. 11. Cathodoluminescence intensity as a function of accelerating voltages: (a) 1, (b) 5, (c) 10, and (d) 15 kV. The film was grown at 4 mTorr, 100 W, and 10% O_2, without substrate heating, followed by annealing at 850°C.

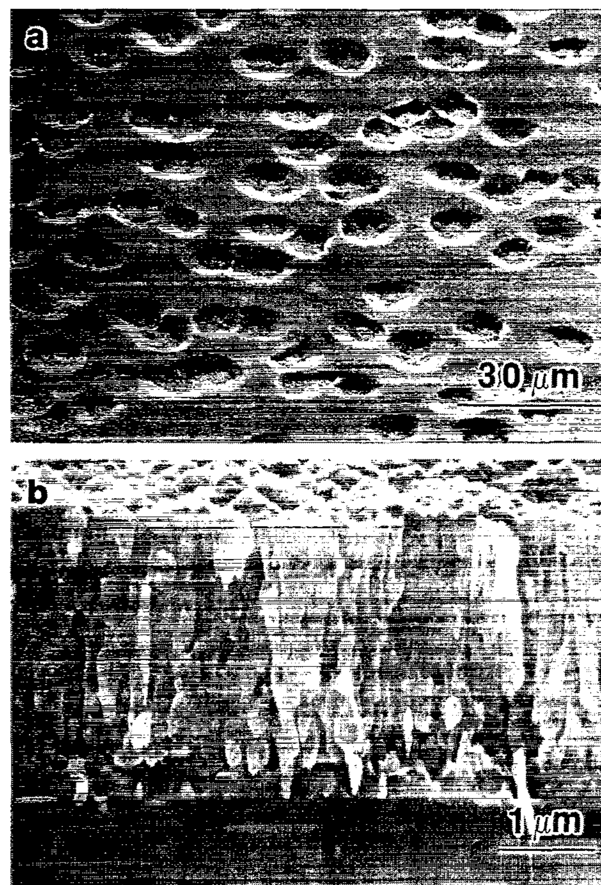

Fig. 12. SEM images of $MgWO_4$ film (4 mTorr, 100 W, 10% O_2, and no substrate heating) taken after annealing at 850°C: (a) planar and (b) cross-sectional views.

4. Conclusions

Uniform and dense $MgWO_4$ thin film phosphors prepared by RF magnetron sputter deposition were obtained and, with

proper post-deposition annealing applied, a desirable cathodoluminescence property could be achieved. α- and β-$MgWO_4$ were found as the major phases in the as-deposited films. Owing to a difference in the cooling rate, the phase formation was apparently determined by the deposition rate of the film. When the film grew at high deposition rates such as high RF power, low working pressure, or low oxygen content, formation of the low-temperature β-$MgWO_4$ phase was favorable. In contrast, low RF power, high working pressure or high oxygen content resulted in relatively low deposition rates and favored the high-temperature α-$MgWO_4$ phase formation. Substrate temperatures showed no noticeable effects on the deposition rates and therefore the β-$MgWO_4$ phase was the only phase present for the substrate temperature range studied. Regardless of the phases present in as-deposited films, the annealing led to a phase transformation and the stable β-$MgWO_4$ phase resulted with better film crystallinity. Consequently, the cathodoluminescence properties were greatly improved after annealing. However, annealing-induced defects such as craters and blisters appeared to deteriorate the LVCL property of film.

Acknowledgements

Professor P. Lin and Mr C.F. Yu of the National Chiao Tung University are gratefully appreciated for assistance in performing sputter depositions and CL measurements. Dr K.S. Chen, Dr K.H. Hsu, and Mr J.N. Yang of the Tatung Institute of Technology are also acknowledged for their assistance during the course of this research. The National Science Council of the Republic of China is gratefully acknowledged for the support under Grant numbers NSC 84-2215-E-216-003 and NSC 85-2216-E-019-004.

References

[1] M.K. Jayaraj, C.P.G. Vallabham, J. Electrochem. Soc. 138 (1991) 1512.
[2] S. Itoh, T. Kimizuka, T. Tonegawa, J. Electrochem. Soc. 136 (1989) 1819.
[3] S. Itoh, H. Toki, Y. Sato, K. Morimoto, T. Kishino, J. Electrochem. Soc. 138 (1991) 1509.
[4] I.J. Hsieh, M.S. Feng, K.T. Kuo, P. Lin, J. Electrochem. Soc. 141 (1994) 1617.
[5] I.J. Hsieh, K.T. Chu, C.F. Yu, M.S. Feng, J. Appl. Phys. 76 (1994) 3735.
[6] J.T. Randall, Br. Patent No. 469732 (1936).
[7] F.A. Kröger, Philips Res. Rep. 2 (1947) 177.
[8] G. Blasse, G.J. Dirksen, M. Hazenkamp, J.R. Günter, Mater. Res. Bull. 22 (1987) 813.
[9] J.R. Günter, M. Amberg, Solid State Ion. Diffus. React. 32-33 (1) (1989) 141.
[10] J.L. Vossen, in: J.L Vossen, W. Kern (Eds.), Thin Film Processes, Academic Press, San Diego, CA, 1978, p. 50.
[11] J.M. Rigsbee, Physical vapor deposition, in: R. Kossowsky (Ed.), Surface Modification Engineering, CRC Press, Boca Raton, FL, 1989, pp. 240–241.
[12] J.P. Chu, C.H. Chung, P.Y. Lee, J.M. Rigsbee, J.Y. Wang, Met. Mater. Trans. 29A (1998) 647.
[13] S.M. Shin, M.A. Ray, J.M. Rigsbee, J.E. Greene, Appl. Phys. Lett. 43 (3) (1983) 249.
[14] B. Cantor, R.W. Cahn, Acta Metall. 24 (1976) 845.
[15] N. Saunders, A.P. Miodownik, J. Mater. Sci. 22 (1987) 626.
[16] J.P. Chu, J.W. Chang, P.Y. Lee, J.K. Wu, J.Y. Wang, Thin Solid Films (1997) in press.
[17] T. Kawashima, H. Taniguchi, H. Kato, F. Yokoyama, K. Shibata, Electroluminescence Proceedings of the Sixth International Workshop, El Paso, TX, USA, 11–13 May 1992, Cinco Puntos Press, 1992, pp. 298–303.
[18] W.A. Bryant, in: R. Kossowsky (Ed.), Surface Modification Engineering, CRC Press, Boca Raton, FL, USA, 1989, p. 204.
[19] A. Fuh, R.P. Gallinger, P. Schuster, J. Adolph, O. Caporaletti, Thin Solid Films 207 (1992) 202.